ICCPGE 2016, 1, 25 - 30

Dynamic Simulation of Performance and Behavior of a "CSP" Parabolic Trough Power Plant with Concrete Storage, If Operated in the South Region of Libya

Gassem A. Azzain[1], Mohamed I. Alowa[2]

[1,2]Energy and Mining Engineering , Sebha University, Sebha , Libya

*Corresponding Author: g_azzain@yahoo.com

Abstract

This paper using (TRNSYS) environment; and through a dynamic simulation approach presents general performance indicators of operation of a proposed Concentrated Solar Power (CSP) plant. The "Parabolic Trough Collector" technology is implemented for electric power generation according to the Rankin cycle for steam generation using the flux of Direct Normal Insolation (DNI). The higher values insolation combined by meteorological environment of the Sahara desert which is available at Longitude 14° E, and Latitude 27° N in the region of "Fazzan" at the south of Libya were the main reasons behind the expected good performance of the system. On the other hand, the storage of the available DNI as heat is selected option to come over the problem of the lack of DNI during night and less expected forecast days. Additional area of mirrors and extended absorbing heat pipes has been considered to collect and convert more solar radiation into heat that has to be stored to cover later power demand. A concrete storage was the choice to store sensible heat for later use. Good performance indicators of solar system and storage behavior have been observed and registered for long term simulation.

Keywords: Concentrated Solar Power CSP Technology, Simulation, Direct Normal Insolation DNI, Solar, Power Generation, Concrete Heat Storage.

1. Introduction

The increasing in human population and activities which causing power demand growing all over the world. The traditional power generation processes based on fossil fuels are no more acceptable as the only solution from the view point of environment, security and economy. Libya as an oil and gas producer is not exception in this context, especially with its plans for large scale development. Increasingly, more power is currently needed to cover these demands. Most previous studies concluded that a program of power mix from conventional and solar sources is the typical solution for its case [1]. The CSP technology has been chosen to produce electrical energy and contribute to the total power mix [2]. The south west region "Fazzan" is one of a high levels of Direct Normal Insolation (DNI) [3]. The daily available solar radiation is coincident with the increase of electrical power demand per day. This issue is strongly related to the effectiveness of solar-thermal energy conversion and storage processes. Economically and environmentally, for large scale power generation; the CSP systems with thermal storage are more recommended over the PV systems because of the relative lower cost of thermal storage against the use of batteries and due to the environmentally friendly production of thermal reservoirs components compared with the manufacturing of batteries. The lower cost of thermal

energy storage possibility is an advantage over the Solar-Photovoltaic energy conversion and storage processes; because of the high cost of batteries. From the cost side view of this subject and according to "Doerte Laing et al"[11], the concrete heat storage has an impressively low cost of $0.78 per kWh, far less than the U.S Department of Energy's goal of $15 per kWh. To give a better idea of how this compares to batteries: Lead-acid batteries cost upwards of $25 per kWh, lithium-ion batteries cost $50 to $100 per kWh. Lithium-ion batteries can last 4 times longer than lead-acid batteries depending on the type and usage [12]. The CSP technology with thermal storage capability would allow for full load coverage; and this will result in total elimination to the partial usage of fossil fuel leading to more compliance with Kyoto protocol and to the later international environmental measures. Solar energy is a variable energy source because of the daily and seasonal changes and clouds cover. However, according to SolarPACES program of the International Energy Agency (IEA), solar power plants designed for solar-only generation are well matched to summer noon peak loads in areas with significant cooling demands, such as Spain or the south-western United States [4] and also in North Africa and the Middle East, although in some locations solar PV does not reduce the need for generation of network upgrades given that air conditioner peak demand often occurs in the late afternoon or early evening when solar output is zero [5] and [6]. SolarPACES states that by using thermal energy storage systems the operating periods of solar thermal power (CSP) stations can be extended to become dispatchable (load following) [4]. The IEA CSP Technology Roadmap (2010) suggests that "in the sunniest countries such as Libya, CSP can be expected to become a competitive source of bulk power in peak and intermediate loads by 2020, and of base-load power by 2025 to 2030" [7] and [8]. A dispatchable source is more valuable than base-load power [9] and [10]. And according to official plans of Renewable Energy Authority of Libya (REAOL) one should know that the targeted share of renewable energy in installed power generation capacity for total energy mix in Libya were to be 6 % in 2015 and are to be 10 % by 2020 [1].

2. Simulation Method

A computer dynamic simulation program has been used to perform this research [14]. A black box analog has been adapted according to the flow chart as shown in figure (2.1), input data are the hourly weather ambient conditions of dry and wet bulb temperatures, relative humidity, wind speed and the insolation (DNI). The data processing elements are the system physical components as shown in figure (3.1) and as represented in figure (6.1), like the solar field, thermal storage "concrete storage, Storage controller" etc.. The load side which consists of steam generators, steam turbine unit, condenser and cooling tower, feed pumps etc. all were replaced by a daily fixed load demand in this simulation and it has been simulated using forcing function of scheduled flow rate through the concrete storage.

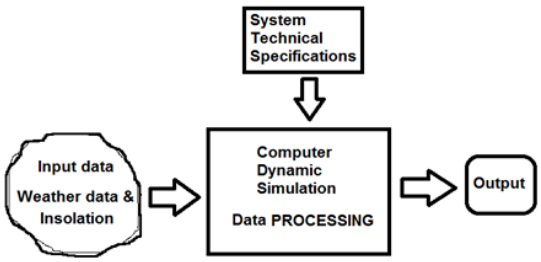

Figure 2.1: Main Processes Flow Chart

The output elements are output data acquisition tools consisted of virtual printers and online plotters to collect the numerical results of the system simulation.

3. The CSP Plant details

The construction of the basic CSP system proposed is shown in figure (3.1). where the main components are the solar collector field of parabolic trough reflectors, steam generators (pre-heater, evaporator, super-heater, and re-heater), double stage steam turbine, the condenser, boiler feed water pump and solar field pump. The proposed construction of the modified CSP system is also shown in figure (3.1). The difference which is the ultimate goal of this research is the elimination of the fossil fuel boiler which replaced by a full concrete storage that has to be a combined by the increase of the area for solar energy collection by (Solar field extension).

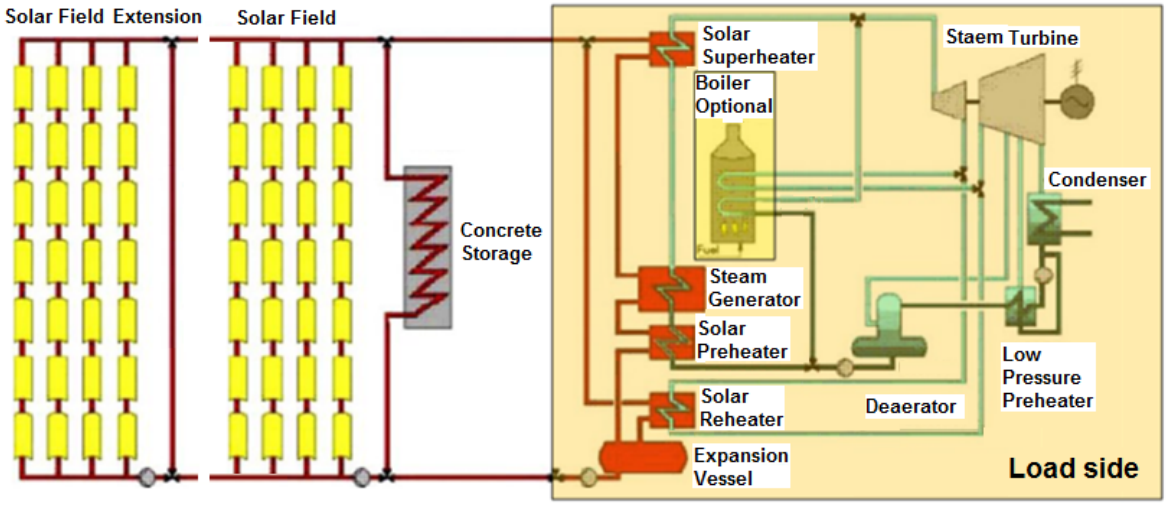

Figure 3.1: Classical CSP Hybrid Power Plant, Concrete Storage and solar field extension [5].

4. Solar Thermal Energy Storage Concept and CSP plant

The heat energy storage concept within the application of CSP technology for electric power generation targeted in this research, is demonstrated as shown in the figure (4.1), [11]; where the extent of the direct contribution of solar heat and stored solar heat additional to the fossil fuel backup value imposed against the required demand represented by the firm capacity line. The ultimate goal within this concept is to cover - as much as possible - the whole expected
load desired by the power plant by using of solar energy only ; this means that the solar energy collection system must capture and convert the required power on dailly bases, and this must be done by increasing the total area of solar collectors; which means that a surplus of that power shuld be stored for later use in the same day. Now, for certain storage volume the question is how much the increase of energy storage percent over the demand for specified increase of the area of a solar field?

5. Simulation Platform

The system main components involved in the simulation process are shown in figure (6.1). In this figure the flow diagram and arrows indicate the transfer of both physical and numerical data for input, processing an output interactions or output registration.

6. Performance criteria

Several parameters and criteria as shown below from equations (1) to (6) have been used - not necessary explicitly - to observe the plant performance as it has been modified from the basic hybrid solar-fuel configuration to the solar thermal storage configuration.

1. Yearly Total Energy Input = Fuel Energy + Solar Energy

   $E_{CSP} = E_{fossil} + E_{solar} = P_{CSP} * CF_{CSP} \cdot 8760$ (MWh/y)

2. Capacity factor = (Net Energy Output / Max Power Output (in a year)) ×100

   $CF_{CSP} = (E_{CSP} / (P_{CSP} \cdot 8760))$ %

3. Gross Conversion Efficiency = Net Energy Output / Total Energy Input

   $\eta_{gross} = (E_{Noutput} / E_{CSP})$ %

4. Storage efficiency = (Heat from Storage / Heat to Storage) × 100

   $\eta_{stor} = (Q_{stor,out} / Q_{stor,in})$ %

5. Solar Contribution= (Solar Energy Input / Total Energy demand) × 100

   $SC = (SE_{input} / TED)$ %

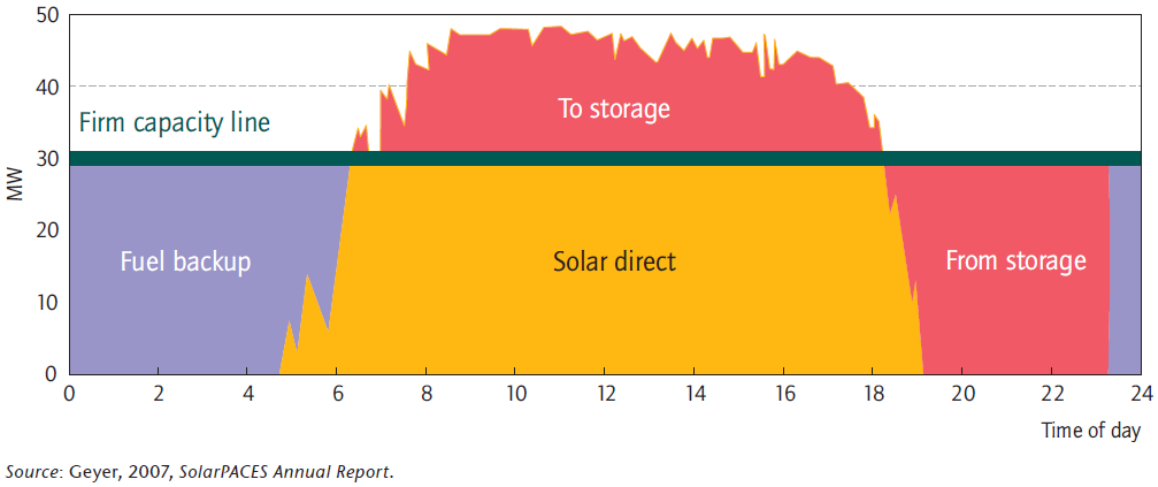

Figure 4.1: Solar Energy Storage Role and Position [5] &[11].

6. Yearly Net Energy Output = Total Energy Input - Total Energy Loss

   $E_{Noutput}$ = E_{CSP} - E_{Loss} (MWh/y)

7. Input Data

Parabolic trough solar field and steam power plant: The general parameters used as numerical data and technical specifications setup to the simulation platform are shown in Table (7.1) and (7.2), where Table (7.2) presents specifically the details of the parabolic trough solar collector with the necessary coefficients to solve numerically the formula for collector efficiency and others.

8. Concrete Storage

It is consisted of large cement blocks similar to that one shown in figure (8.1), [12] connected together in series and parallel arrangement for optimum capacity and HTF flow. The storage system parameters and specifications are as shown below in Table (8.1) and (8.2) for the concrete storage and storage controller respectively. More details and specifications of the concrete storage for solar thermal energy for power generation are presented in [16].

Weather Conditions

Weather data for the south region of Libya and specifically for the area around Sebha that have been used in the simulation were adopted from Meteonorm [13] .

Experimental Validation

The model used to simulate the concrete thermal energy storage described above has
been validated experimentally by Doerte Laing et al. [12], and the results were compared as shown below in figure (8.2). An excellent agreement between the results of the experimental performance and simulation outcomes has been achieved. This agreement was behind the high confidence in the outcomes obtained from the simulation results of this research.

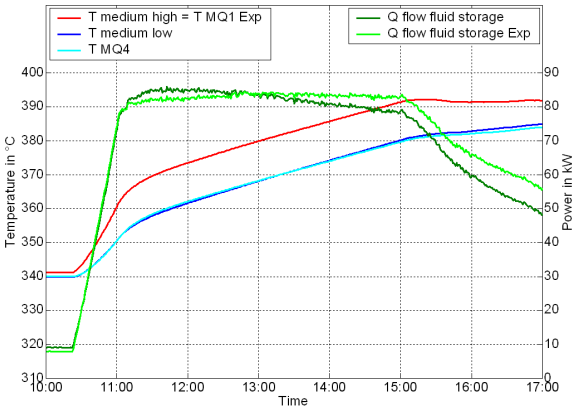

Figure 8.2: Comparison of Simulation and Experiment [12]

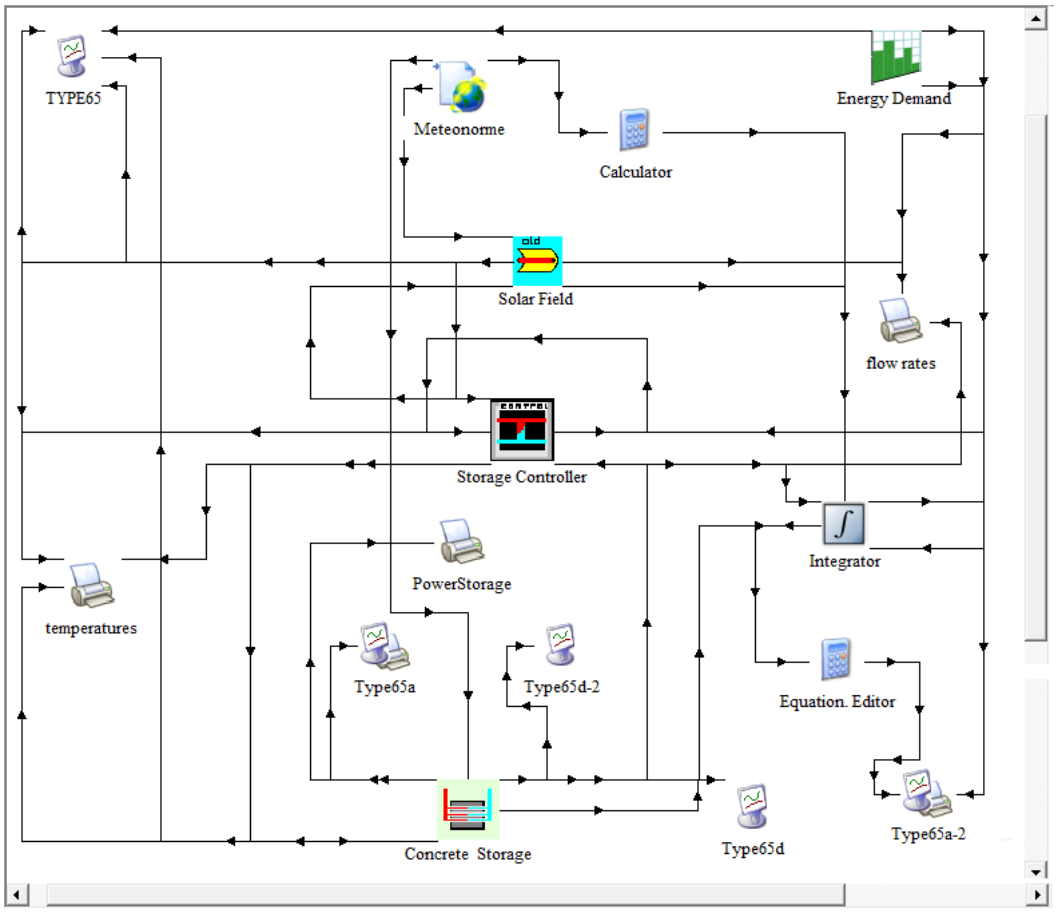

Figure 6.1: Simulation of Data Circulation [14].

Table 7.1: Proposed general specifications for the simulated CSP parabolic trough plant compatible with international standards.

CSP Technology	Parabolic Trough Plant
Unit Capacity (MW)	1 - 100
Unit Solar Concentration	70 - 80
Peak Solar Efficiency (%)	21 ^{D}
Annual Solar Efficiency (%)	10 -15 ^{D}, 17 - 18 ^{P}
Thermal cycle Efficiency (%) (Steam)	30 - 40
Solar Capacity Factor (CF%) as a function of thermal Load	24 ^{D}, 25 - 90 ^{P}
Land use (m2/MWh/y) depending on Solar (CF %)	6 - 8
Area Approx. for each 50 MWe (km2 or ha)	1 or 100
Max Operation Temp (°C)	550 - 390
Expected area km2-For 100 MWe Plant with (CF %)	(24) 1.88 , (90) 5.5

D = Demonstrated, P = Projected.

Table 7.2: Parameters of the Parabolic Trough Solar Collector Assembly (SCA) [14].

(STEC_STORAGE_Sebha_11.tpf) Solar Field

Parameter | Input | Output | Derivative | Special Cards | External Files | Comment

1	A - Loss coef.	**72.0**	-	More...
2	B - Loss coef.	**-0.0071**	-	More...
3	C - Loss coef.	**-1.5022**	-	More...
4	Cw- Loss coef.	**-0.238**	-	More...
5	D - Loss coef.	**-0.06897**	-	More...
6	Clean Reflectivity	0.94	-	More...
7	Broken Mirror Fraction	0.0	-	More...
8	Length of SCA	**99.0**	m	More...
9	Aperature Width of SCA	**5.7**	m	More...
10	Focal Length of SCA	**2.12**	m	More...
11	Rowspacing	**17.3**	m	More...
12	Total Field Area	**100000**	m^2	More...
13	Pump Max Power	**2.16e+006**	kJ/hr	More...
14	Pump Max Flow Rate	**1.5e+006**	kg/hr	More...
15	Pump Power Coeff. 1	1.308	any	More...
16	Pump Power Coeff. 2	4.28E-3	any	More...
17	Pump Power Coeff. 3	1.99E-5	any	More...
18	Tank Heat Loss Rate at 275 C	**1.0e6**	W	More...
19	Piping Heat Loss/Area at 343C	20	W/m^2	More...
20	Field Tracking Parasitics/Area	0.86	W/m^2	More...
21	Field Stow Energy	11250	J	More...
22	Wind Speed Limit for Tracking	13.7	m/s	More...
23	Turn Down Ratio (min flow ratio)	**0.05**	-	More...

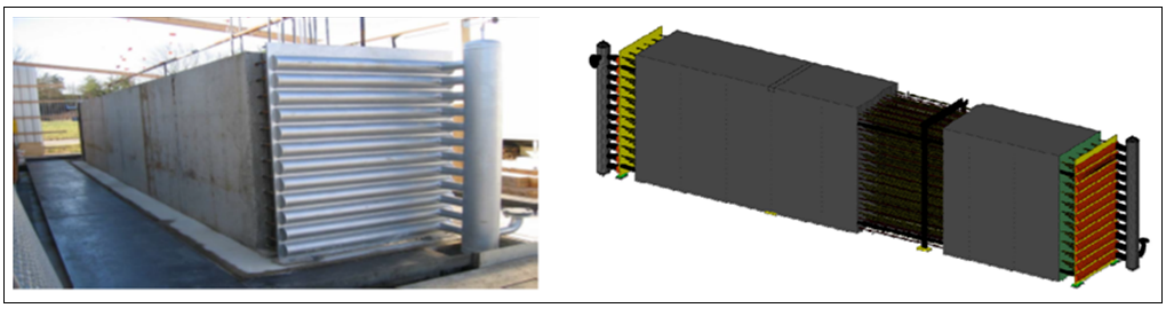

Figure 8.1: Storage Module with Visible Tube Register [12].

Table 8.1: Parameters of the Storage Controller [14].

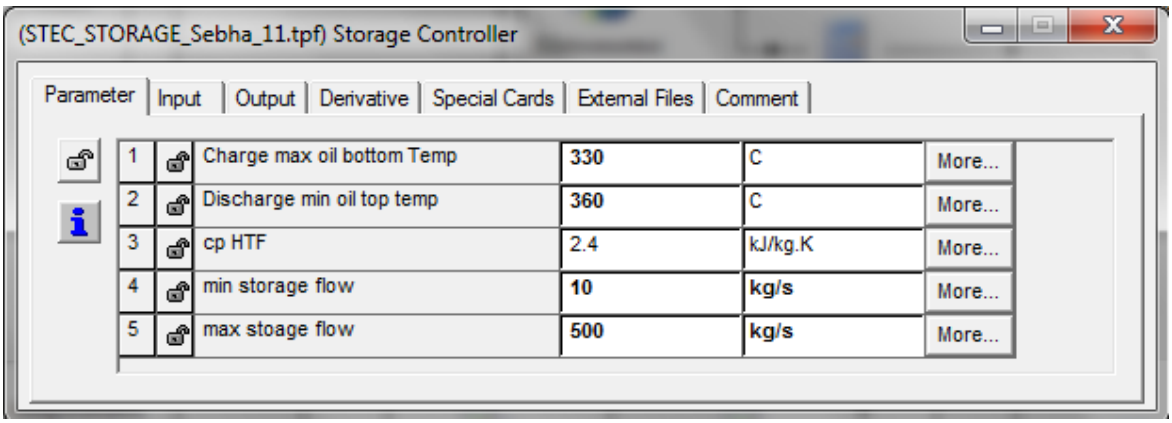

Table 8.2: Parameters of the Storage Controller [14].

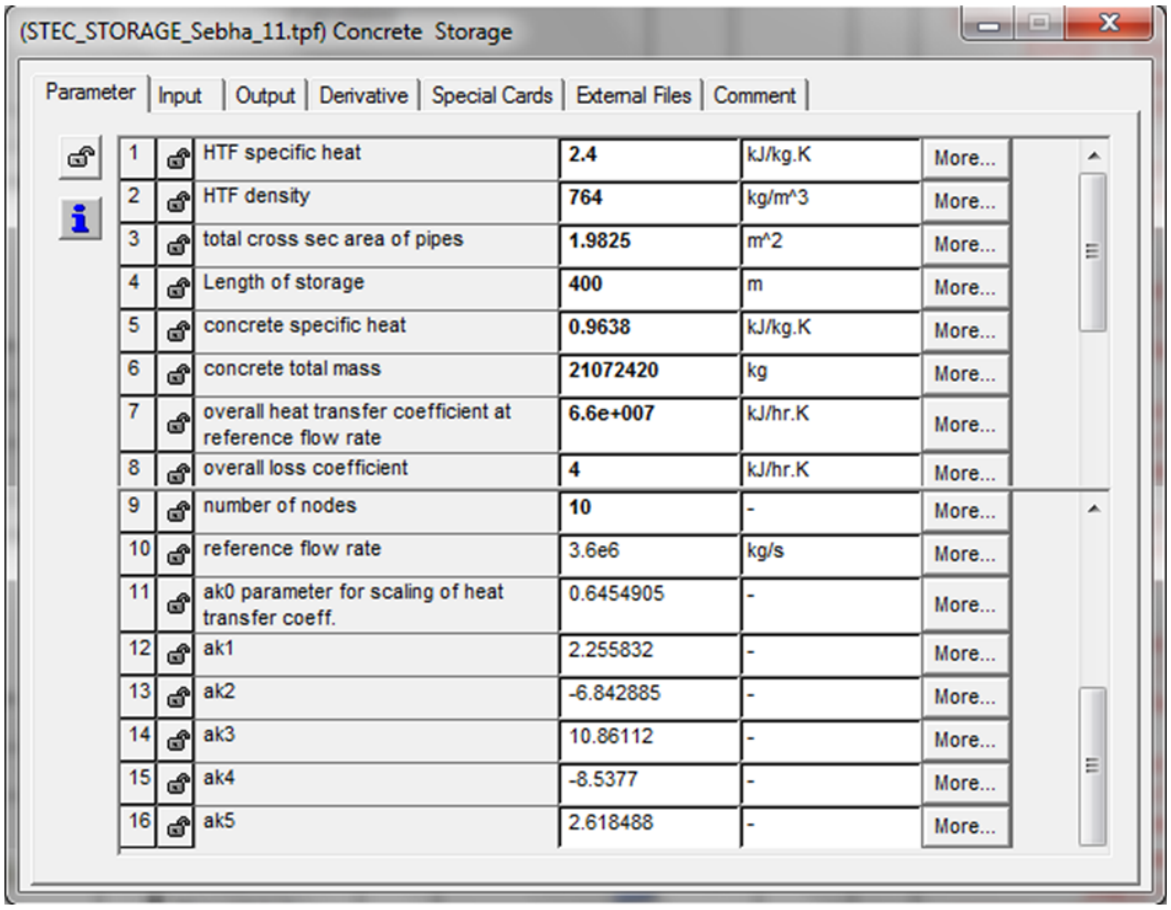

9. Results and Discussion

The following figures have been chosen to present the system general performance and the thermal storage behavior. The four main energy quantities that have been monitored throughout the simulation were:

1. The available solar thermal energy from solar field (DNI) which is dependent on the aperture area,
2. The net solar collected energy that is actually converted to heat after the optical and thermal efficiencies have been applied.
3. The thermal energies charged and discharged of the concrete storage,
4. the total energy lost from the storage.

The criteria for system assessment were

(i) the (Storage Efficiency) %

(ii) (Net Collected Solar Energy to DNI) %

(iii) (Energy from Storage to DNI) %

(iv) the most important (Energy Stored to Energy Demand) %

The energy accumulation for one year is shown in the figure (9.1).

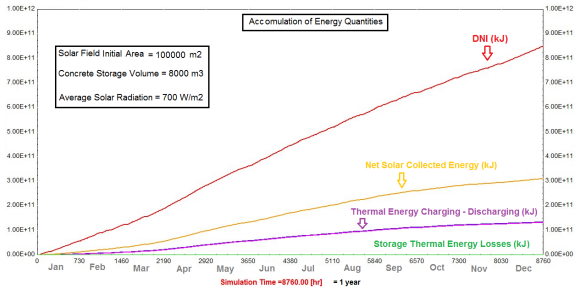

Figure 9.1: Energy Accumulation

The simulation starts with initial area of solar field 100,000 m2, which increased by 100,000 m2 each run to have ratios of (m2 Acoll vs. m3 Vstor) as (25:2, 50:2, 75:2, 100:2, 125:2, and 150:2) with fixed storage volume 8000 m3, while the average solar DNI is 700 W/m2. The effect of charging discharging processes performed for one year according to the previously mentioned plan on the temperature gradient within the storage has been demonstrated in figure (9.2) and a standard behavior of storage material has been reported as seen with maximum temperature difference about 100 °C.

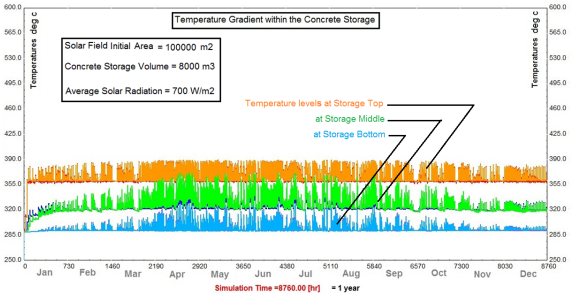

Figure 9.2: Temperature Gradient Across the Concrete Storage from the 1st Simulation Run for One Year.

The impact of the heat charging and discharging of the concrete storage is indicated as temperatures variations between the top and bottom of the storage as in figure (9.3), for days with minimum and maximum solar insolation.

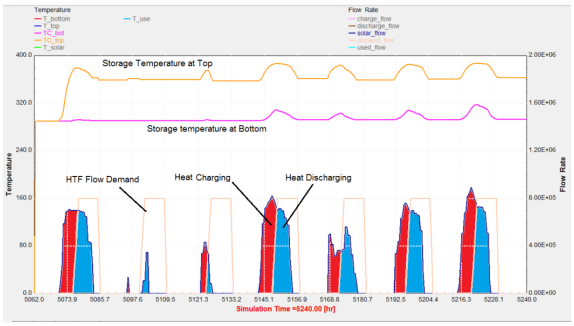

Figure 9.3: Temperature Gradient, HTF Demand and Charging - Discharging Processes Within the Concrete Storage.

Figure (9.4), shows lower percent values of stored energy when matched by demand, about 60 % at (Acoll : Vstor = 25: 2) by the end of the simulated year.
Figure (9.5), at (Acoll : Vstor = 50 : 2) shows increase of the percent values of stored energy when matched by demand, about 120 % in Sep. and over 110 % by the end of the simulated year.

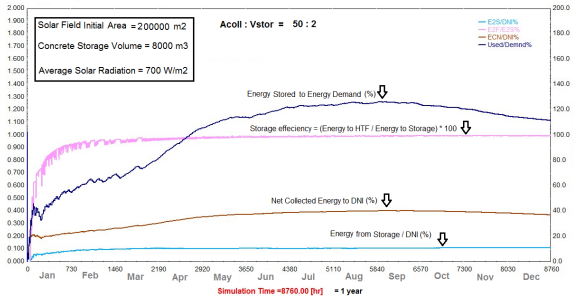

Figure 9.4: 2nd Simulation Run with A_{coll} vs. V_{stor} = 50 m^2 : 2 m^3

Figure (9.6), at (Acoll : Vstor = 75 : 2) shows further increase of the percent values of stored energy when matched with demand, about 160 % in Sep. and about 150 % by the end of the simulated year.

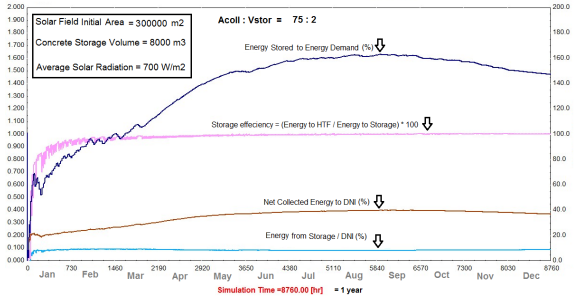

Figure 9.5: 3^{rd} Simulation Run with A_{coll} vs. V_{stor} = 75 m^2 : 2 m^3

Figure (9.7), at (Acoll : Vstor = 100 : 2) shows also further increase of the percent values of stored energy when matched by demand, about 180 % between Aug. and Sep. and about 165 % by the end of the simulated year.

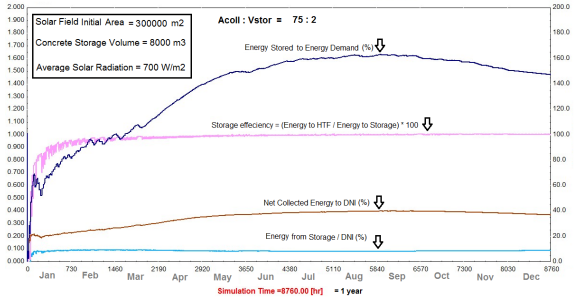

Figure 9.6: 4^{rtd} Simulation Run with A_{coll} vs. V_{stor} = 100 m^2 : 2 m^3

Figure (9.8), at (Acoll : Vstor = 125 : 2) also shows further increase of the percent values of stored energy when matched by demand, maximum about 190 % between Aug. and Sep. and about 175 % by the end of the simulated year.

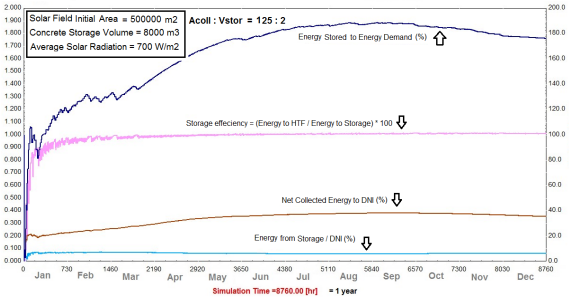

Figure 9.7: 5^{th} Simulation Run with A_{coll} vs. V_{stor} = 125 m^2 : 2 m^3

Figure (9.9), at (Acoll : Vstor = 150 : 2) also shows approximately the ultimate increase of the percent values of stored energy when matched by demand, maximum about 195 % between Aug. and Sep. and more than 180 % by the end of the simulated year.

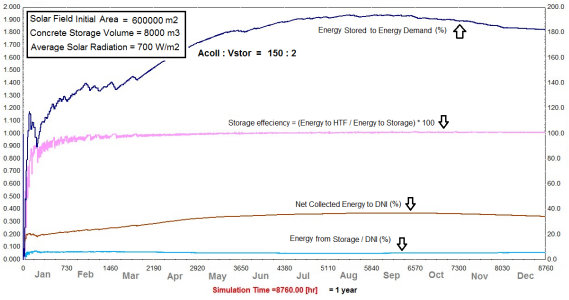

Figure 9.8: 6^{th} Simulation Run with A_{coll} vs. V_{stor} = 60 m^2 : 2 m^3

Figure (9.10), clearly shows the maximum levels of temperature gradients within the concrete storage after the 6th run of the simulation. The ultimate temperature level allowed for the concrete was reached during the summer season and total temperature

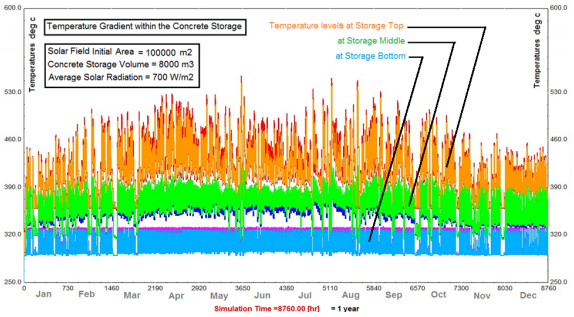

Figure 9.9: Temperature Gradient Across the Concrete Storage from the 6th Simulation Run for One Year.

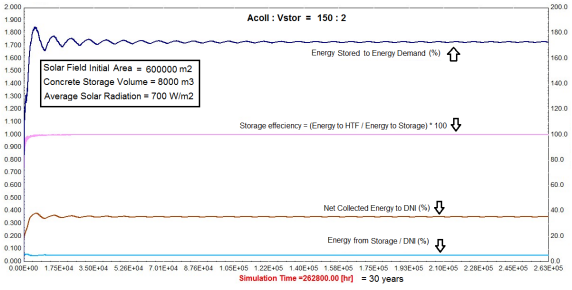

Figure 9.10: Theoretical Steady State Operation of the Storage System for 30 Years Continuously.

difference across the storage was about 160 °C. This may indicate that the storage has reached its safe capacity with an effective thermal storage performance. From the figures above, its noticeable that effect of thermal inertia when the storage has to be started for the first time should be taken into consideration in order to eliminate the low performance signs clearly seen during the first three months of operation. Also it is shown that other criteria of the storage and the solar collection annual efficiencies were almost constant at about 98 % and 40 %, while the percentage of the energy from the storage to the DNI is decreasing from about 17 % to 7 %, that is because of the increase of the solar collection with fixed delivery of energy to the load from the storage. The theoretical long term performance (for 30 years) of the concrete storage has been simulated with simulation data from the 6th run and the results were demonstrated in figure (9.11), where the manner of the recorded oscillations shows that the long term of thermal inertia within the storage will be damped to minimum with the continuous operation. The steady state operation of the storage system under the specifications presented in the last run provides the following values: when the ratio of the solar field area is 150 m^2 to 2 m^3 of storage volume; the percent of stored energy to the demanded energy is about 170 %, this means that there are 70 % more energy stored than the requested energy by demand . This energy surplus in fact should be available for more power generation later during the day after the sun set or during the time of overcast.

10. Conclusion

Mainly, this research has demonstrated the possibility of almost full coverage of energy demand through conversion of solar to thermal energy, storage, up to the consumption series. Taking into account that the choice of the concrete storage was based on expected lower cost compared with other techniques of thermal energy storage; that is if the storage volume or specific thermal capacity of the storage material were not more important. In general, one can see from this theoretical research that the listed main functions required by a storage system within a CSP plant were carried out.
These functions are :

1. Buffering during variable sunshine periods
2. Shifting of time in using available radiation
3. Increment in the annual Capacity Factor.
4. Reduction consequently in the cost of produced energy.
5. production of energy more regularly.
6. Improving dispatch-ability.
7. Utilization more effectively of larger quantities of available solar radiation.

Finally, sustainability conditions and cleaner environment will be secured.

References

[1] Outlook for Electricity and Renewable Energy in Southern and Eastern Mediterranean

Countries Manfred Hafner, Simone Tagliapietra and El Habib El Andaloussi MED-PRO Technical Report No. 16/October 2012.

[2] Thomas R. Mancini and Michael Geyer (2006). Spain Pioneers Grid Connected Solar Tower Thermal Power SolarPACES, OECD/ IEA, p. 3.

[3] R. Ramelli, O. M. Shalabiea, I. Saleh, and J.O. Stenflo, eds. PROSPECTS OF RENEWABLE ENERGY IN LIBYA, Faculty of Engineering, Tripoli University P.O. Box 13656 Tripoli, Libya, International Symposium on Solar Physics and Solar Eclipses (SPSE) 2006.

[4] South Australia's Feed-In Mechanism for Residential Small-Scale Solar Photovoltaic Installations, Government of South Australia (2007), p.13,14 .

[5] International Energy Agency (2010). Technology Roadmap: Concentrating Solar Power p. 5.

[6] Tom Konrad, Ph.D,Why CSP Should Not Try to be Coal. http://www.altenergystocks.com /archives/2009/04/why_csp_should_not_try_to_be_coal.html.

[7] http://en.wikipedia.org/wiki/Capacity_factor.

[8] International Energy Agency (2010). Technology Roadmap: CSP p. 5.

[9] Does Renewable Energy Need to Provide Baseload Power? http://www.altenergystocks.com /archives/2009/04/why_csp_should_not_try_to_be_coal.html.

[10] https://en.wikipedia.org/wiki/Capacity_factor#cite_ref-13.

[11] Laing D., Steinmann W.D., Tamme R. Solid Media Thermal Storage for Parabolic Trough Power Plants. Solar Energy 2006;80 1283–1289.

[12] Laing D., Lehmann D. ; German Aerospace Center, Bahl C., Ed. Züblin AG; "Concrete Storage for Solar Thermal Power Plants", IRES III 2008, 3rd International Renewable Energy Storage Conference, 24.-25.11.2008, Berlin.

[13] Global meteorological database, http://meteonorm.com.

[14] TRNSY the Transient Systems Simulation Program, http://www.trnsys.com

[15] Mohamed R.Zaroug "Renewable Energy in Libya (The Future Prospectives)" Renewable Energy Authority of Libya (REAoL), Wednesday 28th of March 2012, Amman, Jordan.

[16] V. A. Salomoni, C. E. Majorana, G. M. Giannuzzi, R. Di Maggio, F. Girardi, D. Mele and M. Lucentini, "Conceptual Study of a Thermal Storage Module for Solar Power Plants with Parabolic Trough Concentrators". http://dx.doi.org/10.5772/54060